Time-Dependent Density Fluctuations in a Strongly Coupled Ionic Mixture

I. R. McDonald
Department of Chemistry, Royal Holloway College, Egham, Surrey, England

and

P. Vieillefosse and J. P. Hansen
Laboratoire de Physique Théorique des Liquides,[a] *Université Pierre et Marie Curie, 75230 Paris Cedex 05, France*

(Received 13 June 1977)

Hydrodynamic and molecular-dynamics calculations show that the charge fluctuations in a strongly coupled H^+-He^{++} mixture are dominated by a propagating plasmon mode which is damped by interdiffusion even in the long-wavelength limit. A sum-rule argument indicating that the plasmon dispersion changes from positive to negative as the coupling increases is consistent with both kinetic theory and the computer results. Plasma oscillations also contribute weakly to the mass fluctuations, but there is no hydrodynamic sound-wave mode.

The system we consider is that of a fluid mixture of two species of positively charged ions, of charges Z_1e and Z_2e and masses M_1 and M_2, immersed in a uniform, rigid, neutralizing background of degenerate electrons, in a range of temperature and density such that the ions can be treated classically. This is a natural generalization of the widely studied classical one-component plasma (OCP); for convenience we shall therefore refer to the binary mixture as a two-component plasma (TCP). The static properties of the TCP are by now accurately known[1] and for given values of Z_1 and Z_2 they depend on only two variables, the concentration $x_1 = N_1/N$ (where $N = N_1 + N_2$ is the total number of ions) and the dimensionless coupling parameter

$$\Gamma = e^2/ak_BT, \tag{1}$$

where $a = (3/4\pi\rho)^{1/3}$ is the ion-sphere radius, $\rho = N/V$ being the total number density.

In this Letter we report the results of a study of the time-dependent fluctuations in charge and mass densities in a strongly coupled TCP by (i) a hydrodynamic calculation and (ii) a molecular-dynamics (MD) "experiment," adopting as the unit of time the inverse of the plasma frequency

$$\omega_p = (4\pi\rho\bar{Z}^2e^2/\bar{M}^2)^{1/2}, \tag{2}$$

with $\bar{Z} = x_1Z_1 + x_2Z_2$ and $\bar{M} = x_1M_1 + x_2M_2$. The quantities of primary interest are the autocorrelation functions of the densities of charge ($A = Z$) and mass ($A = M$), i.e.,

$$F_{AA}(q, t) = (1/N\bar{A}^2)\langle \rho_A(\vec{q}, t)\rho_A(-\vec{q}, 0)\rangle, \tag{3}$$

where $\vec{q} = a\vec{k}$ is a dimensionless wave vector and

$$\rho_A(\vec{q}, t) = \sum_{j=1}^{N} A_j \exp[-i\vec{q}\cdot\vec{r}_j(t)]. \tag{4}$$

The spectra of fluctuations in the densities are described by the Fourier transforms

$$S_{AA}(q, \omega) = (1/2\pi)\int_{-\infty}^{\infty} F_{AA}(q, t)\exp(i\omega t)\,dt \tag{5}$$

with frequency moments defined as

$$\overline{\omega_{AA}^{2n}(q)} = \int_{-\infty}^{\infty} \omega^{2n} S_{AA}(q, \omega)\,d\omega. \tag{6}$$

To obtain information on the character of mass and charge fluctuations in the long-wavelength, low-frequency limit we have computed the power spectra (5) by solving the linearized hydrodynamic equations for $\rho_Z(\vec{q}, t)$ and $\rho_M(\vec{q}, t)$, averaging over initial conditions in the framework of thermodynamic fluctuation theory. Similar calculations have previously been reported for the OCP[2] and for binary molten salts.[3,4] The hydrodynamic equations expressing conservation of charge, mass, momentum, and energy are, in fact, identical to those applying in the latter case, but the process of *linearizing* the Navier-Stokes equation now leads to a different result. The α component ($\alpha = x, y, z$) of the Navier-Stokes equation for charged systems has the general form

$$\rho_M\left(\frac{\partial}{\partial t} + \vec{v}\circ\nabla\right)v_\alpha = \frac{\partial P}{\partial r_\alpha} + \frac{\partial \sigma_{\alpha\beta}'}{\partial r_\beta} + e\rho_Z E_\alpha, \tag{7}$$

where ρ_M is the mass density, $\vec{v}$ is the velocity, P is the pressure, $\sigma_{\alpha\beta}'$ is the dissipative part of the stress tensor, and $\vec{E}$, the electric field, is related to the charge density $e\rho_Z$ by Poisson's equation; the last term on the right-hand side

represents the contribution from the electric force. If we write $\rho_z = \rho_z^0 + \delta\rho_z$, where $\rho_z^0 = NZ/V$ is the equilibrium density of mobile charge carriers, it is clear that $\vec{E}$ is of order $\delta\rho_z$. A molten salt is characterized by the fact that $\rho_z^0 = 0$. Thus the electric-force term in (7) is proportional to $(\delta\rho_z)^2$ and disappears upon linearization. In the case of the TCP, however, the mobile charge carriers are all of the same sign and ρ_z^0 is nonzero; the electric force is therefore linear in $\delta\rho_z$, a result true also of the OCP.

Omitting the technical details, we now summarize the main findings of the hydrodynamic calculation. The determinant of the hydrodynamic matrix has two zeros at imaginary frequencies, corresponding to nonpropagating modes linked to interdiffusion and thermal diffusion, and two at a pair of complex conjugate frequencies, corresponding to damped, propagating plasmon modes. The diffusive poles contribute two Lorentzians of height $O(q^0)$ and width $O(q^2)$ to the normalized charge fluctuation spectrum $\sigma_{zz}(q, \omega) = S_{zz}(q, \omega)/S_{zz}(q)$, where $S_{zz}(q) = \omega_{zz}^{\ 0}(q)$ is the static charge structure factor. The contribution to $\sigma_{zz}(q, \omega)$ coming from the plasmon poles, for $\omega > 0$ and $q \to 0$, is

$$\sigma_{zz}^{\ p}(q, \omega) = \frac{2\omega^2\omega_d}{(\omega^2 - \omega_p^{\ 2})^2 + \omega^2\omega_d^{\ 2}}, \qquad (8)$$

where $\omega_d = 4\pi e^2\alpha$, with α the interdiffusion coefficient.[3] These results differ in two main respects from those obtained for the OCP. First, although in both systems the plasmon mode dominates in the hydrodynamic limit, the plasmon peak in the TCP, unlike that in the OCP, remains of *finite* width and height ($\sim q^0$) as $q \to 0$. Second, the ratio of the plasmon-peak height to the height of the central peak is $O(q^{-2})$ in the OCP but $O(q^0)$ in the TCP. This opens up the possibility of observing the diffusive contribution to the charge spectrum in a MD experiment on the TCP, whereas the central peak has proved undetectable in similar calculations for the OCP.[5] It should be noted that the plasmon mode is not a genuine hydrodynamic mode[6] since it has a finite lifetime and nonzero frequency in the limit $q \to 0$. As in the case of the OCP,[2] however, the plasma frequency is small compared to the collision frequency in the strong-coupling limit ($\Gamma \gg 1$) and the assumption of local thermodynamic equilibrium should be well satisfied.

By contrast, the normalized mass fluctuation spectrum $\sigma_{MM}(q, \omega)$ is made up of a dominant central peak of height $O(q^{-2})$ and width $O(q^2)$, stemming from the imaginary poles associated with interdiffusion and thermal diffusion, and two weak plasmon peaks centered at $\pm\omega_p$, of height $O(q^2)$ and width $O(q^0)$. The integrated intensity of the latter is therefore negligible compared to that of the central peak in the limit $q \to 0$, a behavior which is the exact opposite of that seen in $\sigma_{zz}(q, \omega)$. There is no mode corresponding to a propagating sound wave.

In order to check the extent to which these findings are applicable at shorter wavelengths, we

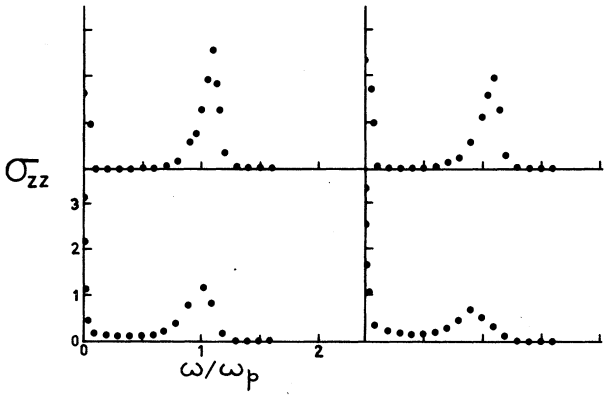

FIG. 1. Spectrum of charge-density fluctuations observed in a MD experiment on a H^+-He^{++} mixture at $\Gamma = 40$. From left to right and top to bottom: $q = 0.6187$, 0.8750, 1.3835, and 1.8562.

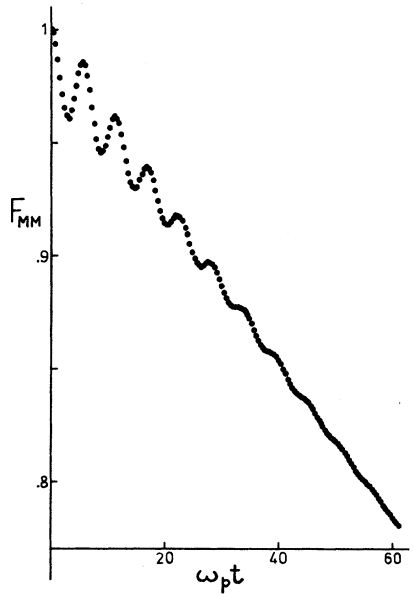

FIG. 2. Mass-density autocorrelation function for $q = 0.6187$ observed in a MD experiment on a H^+-H^{++} mixture at $\Gamma = 40$. The data have been normalized to unity at $t = 0$.

have carried out an extensive MD calculation on a strongly coupled ($\Gamma = 40$) mixture of 125 H^+ and 125 He^{++} ions in a periodically repeating cubic cell. Some of our results are displayed in Figs. 1 and 2.

Figure 1 shows the charge spectrum $\sigma_{ZZ}(q, \omega)$ at four values of q, including the smallest compatible with the periodic boundary condition. Qualitatively the shape of the spectra agree well with the predictions of hydrodynamics: There is a sharp central peak and a broader peak centered near ω_p, the latter being dominant at small q. The position of the maximum in the plasmon peak shows a negative dispersion; i.e., it shifts to lower frequencies with increasing q. Extrapolating to infinite wavelength we find a peak position $\omega_m(q \to 0) \simeq 1.07\omega_p$, somewhat above the hydrodynamic result, $\omega_m(q \to 0) = \omega_p$ [cf. Eq. (8)]; a similar extrapolation of the peak width yields, via (8), the estimate $\omega_d \simeq 0.086\omega_p$.

An approximate dispersion relation [$\omega_m(q)$ as function of q] for the plasmon mode can be based on the q dependence of the second and fourth moments of $S_{ZZ}(q, \omega)$, which in turn can be expressed in terms of the three partial pair distribution functions $g_{\nu\mu}(r)$ ($\nu, \mu = 1, 2$). A straightforward calculation yields

$$\omega_m^2(q) \simeq \overline{\omega_{ZZ}^4(q)}/\overline{\omega_{ZZ}^2(q)} = \omega_m^2(0) + \delta q^2 + O(q^4), \tag{9}$$

with

$$\omega_m^2(0)/\omega_p^2 = \frac{(x_1 z_1^2/m_1 + x_2 z_2^2/m_2)^2 + \frac{1}{3} x_1 x_2 z_1 z_2 (z_1/m_1 - z_2/m_2)^2}{x_1 z_1^2/m_1 + x_2 z_2^2/m_2}, \tag{10}$$

$$\delta(\Gamma \bar{Z}^2/\omega_p^2) = \frac{x_1 z_1^2/m_1^2 + x_2 z_2^2/m_2^2 + \frac{2}{15}\sum_\nu \sum_\mu x_\nu x_\mu G_{\nu\mu}(z_\nu z_\mu/m_\nu m_\mu)}{x_1 z_1^2/m_1 + x_2 z_2^2/m_2}, \tag{11}$$

where $z_\nu = Z_\nu/\bar{Z}$, $m_\nu = M_\nu/\bar{M}$, and

$$G_{\nu\mu} = \int_0^\infty [g_{\nu\mu}(r) - 1] r \, dr \tag{12}$$

with r in units of a. For $x_1 = x_2 = \frac{1}{2}$ we find $\omega_m(0) = 1.076\omega_p$ (independent of Γ!), in remarkably good agreement with the extrapolation of the MD results. Using the $g_{\nu\mu}(r)$ reported previously,[1] we find that δ becomes negative for $\Gamma \gtrsim 1$, implying that the dispersion changes from positive to negative. A similar result applies for the OCP.[5]

The MD results on $\sigma_{MM}(q, \omega)$ show that the spectrum is essentially broad and featureless, with a peak at $\omega = 0$; any structure which may exist near the plasma frequency is undetectable above the noise. However, a detailed analysis of the mass autocorrelation function $F_{MM}(q, t)$ shows that the short-time behavior at small q consists of a weak oscillation at roughly the plasma frequency superimposed on a slow monotonic decay; an example is plotted in Fig. 2. The oscillations correspond to the weak plasmon peak in $\sigma_{MM}(q, \omega)$, a feature predicted by the hydrodynamic calculation.

It is instructive to compare the hydrodynamic and MD results with those obtained in the kinetic regime or weak-coupling limit, i.e., $\Gamma \ll 1$. The charge response function, related to $\sigma_{ZZ}(q, \omega)$ by the fluctuation-dissipation theorem, can easily be obtained by solving the coupled, linearized Vlasov equations for the one-particle distribution functions of the two species of ions. In this approximation the spectrum $\sigma_{ZZ}(q, \omega)$ reduces to a δ function in the limit $q \to 0$, with a dispersion relation given by

$$\omega_m^2(q) = \Omega_p^2 + dq^2, \tag{13}$$

with $d > 0$ and

$$\Omega_p^2 = 4\pi\rho e^2 (x_1 Z_1^2/M_1 + x_2 Z_2^2/M_2). \tag{14}$$

Thus the dispersion is positive, in agreement with (9), and in the long-wavelength limit the plasmon peak is shifted to Ω_p, i.e., a frequency greater than the natural plasma frequency, in agreement with (10). In fact, for the H^+-He^{++} mixture with $x_1 = x_2 = \frac{1}{2}$, $\Omega_p \simeq 1.054\omega_p$. This is similar to the shift observed in the MD experiment, though at $\Gamma = 40$ we are very far from the kinetic regime. The hydrodynamic calculation is in other respects in satisfactory agreement with the MD results, but it fails to predict any such shift. Clearly it would be of interest to extend the MD experiment to lower values of Γ, and we shall report on such calculations elsewhere.

This work has been supported in part by the United Kingdom Science Research Council.

[a]Equipe associé au Centre National de la Recherche

Scientifique.
[1]J. P. Hansen, G. M. Torrie, and P. Vieillefosse, to be published.
[2]P. Vieillefosse and J. P. Hansen, Phys. Rev. A 12, 1106 (1975).
[3]P. Vieillefosse, J. Phys. (Paris) 38, L43 (1977).
[4]P. V. Giaquinta, M. Parrinello, and M. P. Tosi, Phys. Chem. Liq. 5, 305 (1976).
[5]J. P. Hansen, I. R. McDonald, and E. L. Pollock, Phys. Rev. A 11, 1025 (1975).
[6]This point is discussed by M. Baus, Physica (Utrecht) 79A, 377 (1975).

Fast-Ion Generation by Ion-Acoustic Turbulence in Spherical Laser Plasmas

P. M. Campbell, R. R. Johnson, F. J. Mayer, L. V. Powers, and D. C. Slater
KMS Fusion, Inc., Ann Arbor, Michigan 48106
(Received 19 May 1977)

Numerical hydrodynamic simulations which include absorption and transport modifications due to ion-acoustic turbulence have been performed. These simulations can reproduce the important features of the fast-ion velocity distributions as measured with biased charge collectors and a magnetic spectrograph in spherically illuminated microballoon experiments. Experiments with hemispherical targets show that a substantial amount of fast-ion energy is directed inward and may contribute to driving the implosion.

Measurements of ion expansion energy from laser-heated plasmas show an anomalous fast-ion component.[1] Charge collectors biased to record ion current as a function of time show that in a typical experiment approximately half of the absorbed energy resides in only a few percent of the target mass.[2] This result implies that the absorbed energy is being coupled into a very thin layer at the target surface. This mode of coupling leads to poor momentum transfer between the expanding plasma and the compressed region of the pellet and could place a fundamental limitation on the efficiency of laser-driven ablative compression.

Figure 1 presents data from two instruments used to obtain the ion velocity distribution. The target for this laser shot was a 54-μm-diam spherical glass shell with 0.8-μm wall thickness filled with 10 atm of DT gas mixture. The laser energy on the target was 21 J at 1.06-μm wavelength in a 70-psec flat pulse. A lens–ellipsoidal-mirror illumination system provided near-normal illumination of the pellet.[3]

Figure 1(a) shows the voltage trace from a conventional charge collector. The initial sharp spike is produced by photoelectron emission from the collector surface due to the ultraviolet and x-ray flash when the laser pulse hits the target. The second peak results from the fast ions, and the broad feature represents the arrival of the bulk of the ionized target material. Using previously measured values for the mean ionic charge and secondary-emission coefficient,[4] this voltage trace can be converted into an ion-velocity spectrum. Because of uncertainty in the secondary-emission correction, the velocity spectrum above 2×10^8 cm/sec is obtained with a small magnetic spectrograph which uses cellulose nitrate foils as detectors.[5]

Figure 1(b) shows the ion-velocity spectrum. At high velocities, the spectrum is adequately

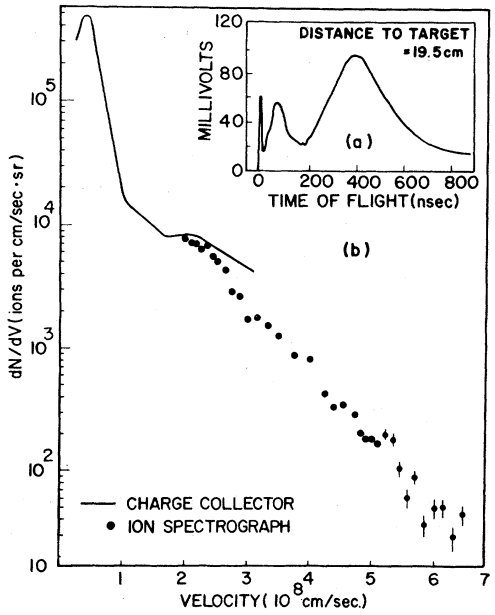

FIG. 1. (a) Oscilloscope voltage trace from a biased charge collector. (b) Composite ion-velocity spectrum from a charge collector and ion spectrograph.